A Sharp Cartesian Method For The Simulation Of Flows With High Density Ratios

Lisl Weynans

Bordeaux University and INRIA, France

3 June 2016

Incompressible flows with high density ratios ?

Air-water interfaces

Context

- NaSCar : 3D parallel incompressible code with fluid-structure interaction
  (Michel Bergmann, INRIA Bordeaux)
- Discretization on cartesian grids, level-set method
- Second-order for velocity near solid boundary : use of ghost cells
  (Mittal et al 2008, Bergmann et al 2014)

Goal : Fluid-structure interaction with waves

Goal : Fluid-structure interaction with waves

Regularized method for interface treatment : CSF

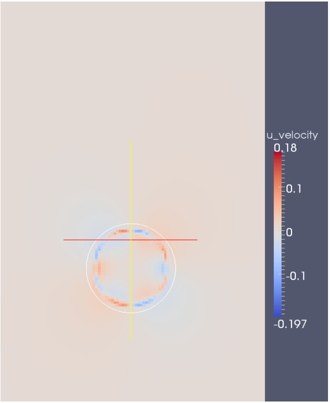

- Loss of accuracy + stability issues
- How to improve the accuracy near the interface ?

$\Rightarrow$ Use a sharp cartesian method to solve the pressure at the interface

Methodology

We work with :

- a discretization on cartesian grids,
- finite differences,
- a level-set function to represent the interface.

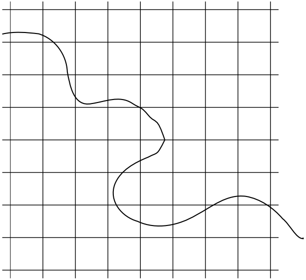

We want

- a second-order accuracy for the pressure
- a scheme easy to implement (and to parallelize)

- The level-set function ϕ is advected with fluid velocity,
- Straightforward treatment of complex geometries and topological changes (fragmentation, coalescence)
- Convenient for discretization on cartesian grids
- Formulas for geometric quantities :

$$\boldsymbol{n} = \nabla\phi, \qquad \kappa = \nabla\cdot\left(\frac{\nabla\phi}{|\nabla\phi|}\right),$$

- In pratice, ϕ is the signed distance to the interface ($\Rightarrow |\nabla\phi| = 1, \;\; \kappa = \Delta\phi$).

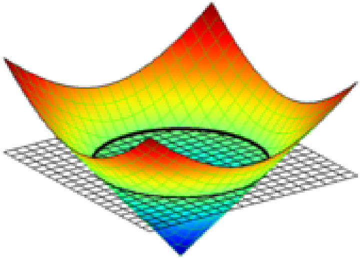

Outline

1. Second-order cartesian method for elliptic problems with immersed interfaces
2. Application to incompressible bifluid flows
3. How to preserve high-order level-set along time ?

Elliptic problem with immersed interface

$$
\begin{aligned}
\nabla.(k\nabla u) &= f \text{ on } \Omega = \Omega_1 \cup \Omega_2 \\
[\![u]\!] &= \alpha \text{ on } \Sigma \\
[\![k\frac{\partial u}{\partial n}]\!] &= \beta \text{ on } \Sigma \\
u &= g \text{ on } \delta\Omega
\end{aligned}
$$

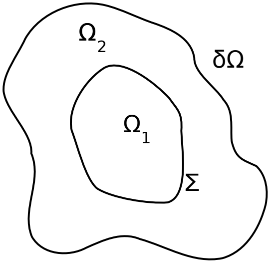

Discretization strategy

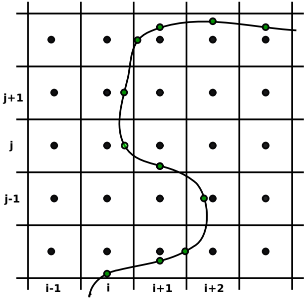

- Creation of additionnal unknowns on the interface
  - used to discretize the elliptic operator on each side of the interface
  - obtained by a discretization of jump conditions across the interface

  A method related to the large family of methods inspired by IIM

- Cons : additional unknowns...
- Pros : additional unknowns !

Which accuracy near the interface ?

To obtain second-order convergence (L^∞ norm), it is enough to have :

- a first-order truncation error for the elliptic operator near the interface
  $\Rightarrow$ avoid linear extrapolations
- a second-order truncation error for the flux discretization
  $\Rightarrow$ use of a larger stencil

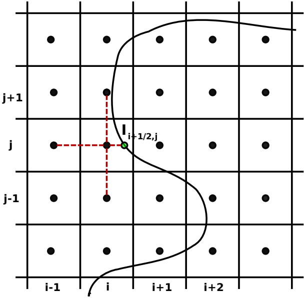

- A_h matrix of linear system, U_h solution, f_h source term

$$A_h U_h = f_h$$

- Local error e_h and truncation error τ_h linked by

$$A_h e_h = \tau_h$$

- Naive estimate :

$$||e_h||_\infty \leq ||A_h^{-1}||_\infty ||\tau_h||_\infty$$

- Not accurate enough here because $||\tau_h||_\infty = O(h)$

$\Rightarrow$ we need bounds on A_h^{-1} coefficients, summed by blocks

- For each discretization point Q, define the discrete Green function $G_h(P,Q)$ as :

$$\left\{\begin{array}{l} A_h G_h(P,Q) = \left\{\begin{array}{ll} 0, & P \neq Q \\ 1, & P = Q \end{array}\right. \\ G_h(P,Q) = 0, \quad P \text{ on the boundary }. \end{array}\right.$$

- Each array $G_h(:,Q)$ is a column of A_h^{-1}

$$u_h(P) = \sum_Q G_h(P,Q)\,(A_h U_h)(Q) \quad \forall P$$

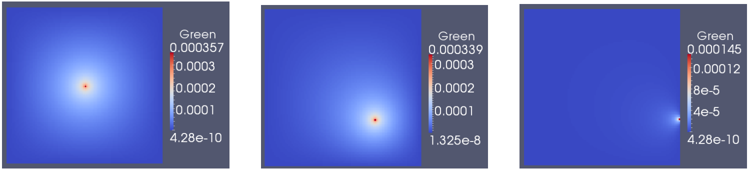

FIGURE: Examples of discrete Green functions

Theorem (Ciarlet, 71) :

S is a subset of Ω_h and W an array such that :

$$\left\{\begin{array}{c} W(P) \geq 0 \quad \forall P \in \Omega_h, \\ (A_h W)(P) \geq 0 \quad \forall P \in \Omega_h, \\ (A_h W)(P) \geq h^{-i} \text{for each } P \in S. \end{array}\right.$$

If A_h is monotonic then

$$\sum_{Q \in S} G_h(P,Q) \leq h^i W(P).$$

Theoretical convergence

- Prove that the matrix is monotonic, that is $(A_h U_h \geq 0 \Rightarrow U_h \geq 0)$:

  requires to prove that if the minimum of U_h is located on the interface, then the discrete flux on this point is negative
- Use discrete maximum principle and ad hoc test functions to obtain bound on the coefficients of $A_h^{-1} = G_h$:

$$\begin{aligned}
\sum_{Q \in \Omega_h^* \cup \Sigma_h} G_h(P,Q) &\leq O(1), \\
\sum_{Q \in \Omega_h^{**}} G_h(P,Q) &\leq O(h^2).
\end{aligned}$$

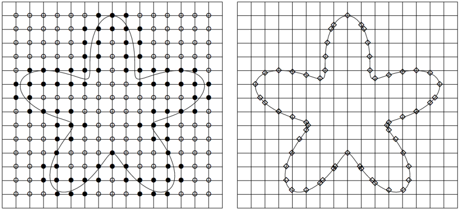

Figure 3: Left: regular nodes (belonging to Ω_h^{**}) described by bullets $\bullet$, irregular nodes (belonging to Ω_h^{**}) described by circles $\circ$:, right: nodes belonging to Σ_h.

Theoretical convergence

- Multiply the truncation error array by A_h^{-1}, block by block :

$$|e_h(P)| \leq \sum_{Q\in\Omega_h^{**}} |G_h(P,Q)\tau_h(Q)| + \sum_{Q\in\Omega_h^{*}\cup\Sigma_h} |G_h(P,Q)\tau_h(Q)|,$$
$$\leq O(h^2)O(1) + O(1)O(h^2) = O(h^2)$$

- In our case :
  - Proof ok in 1D, 2D order 1
  - 2D order 2 : the monotonicity of the matrix depends on the direction of the normal to the interface compared to the direction of the normal to the cartesian cell
  - But monotonicity ensured if normal aligned with the axis of the grid $\Rightarrow$ useful in the bifluid case !

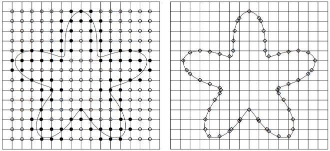

Figure 3: Left: regular nodes (belonging to Ω_h^{**}) described by bullets •, irregular nodes (belonging to Ω_h^{**}) described by circles ○:, right: nodes belonging to Σ_h.

2D convergence test

Interface Σ :

$$(\frac{x}{18/27})^2 + (\frac{y}{10/27})^2 = 1.$$

Exact solution :

$$u(x,y) = \begin{cases} e^x cos(y), & \text{inside } \Sigma \\ 5e^{-x^2-\frac{y^2}{2}}, & \text{outside.} \end{cases}$$

$k = 1$ outside Σ and 10 or 1000 inside.

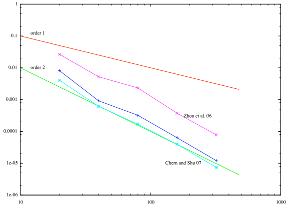

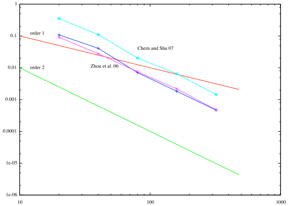

FIGURE: Left : $k = 10$, right : $k = 1000$, convergence in L^∞ norm

Parallel 2D convergence test

$$k = \begin{cases} k^- & \text{inside } \Sigma \\ 1 & \text{outside} \end{cases}$$

$$u = \begin{cases} e^x cos(y), & \text{inside } \Sigma \\ 5e^{-x^2 - \frac{y^2}{2}}, & \text{outside.} \end{cases}$$

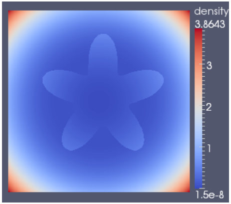

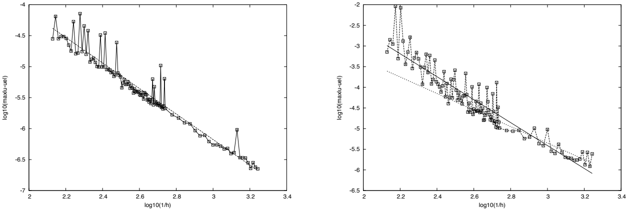

FIGURE: Convergence tests with $\omega = 5$, $r_0 = 0.5$, $k^- = 1000$ (left), and $\omega = 12$, $r_0 = 0.4$, $k^- = 100$ (right).

1. Second-order cartesian method for elliptic problems with immersed interfaces
2. Application to incompressible bifluid flows
3. How to preserve high-order level-set along time ?

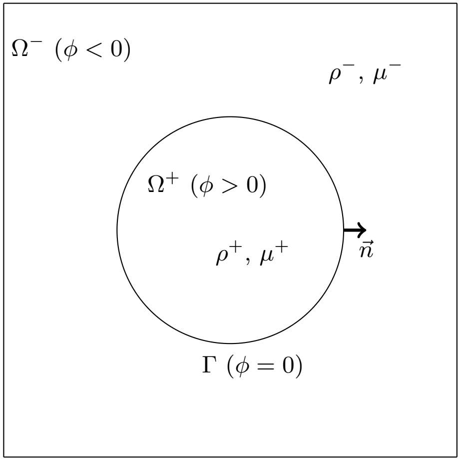
$\Omega^- \ (\phi < 0)$
$\rho^-,\ \mu^-$
$\Omega^+ \ (\phi > 0)$
$\rho^+,\ \mu^+$
$\vec{n}$
$\Gamma \ (\phi = 0)$

Fluid model

- Incompressible Navier-Stokes equations in each fluid :

$$\rho(\boldsymbol{u}_t + (\boldsymbol{u} \cdot \nabla)\boldsymbol{u}) = -\nabla p + (\nabla . \tau)^T + \rho \boldsymbol{g},$$
$$\boldsymbol{\nabla} \cdot \boldsymbol{u} = 0$$

- Jump conditions on Γ :
  - ⋆ Continuity of velocity and divergence of velocity

$$[u] = [v] = 0,$$
$$[(u_n, v_n).\boldsymbol{n}] = 0.$$

  - ⋆ Balance between normal stresses and surface tension

$$[\mu(u_n, v_n).\boldsymbol{\eta} + \mu(u_\eta, v_\eta).\boldsymbol{n}] = 0,$$
$$[p] = \sigma\kappa + 2[\mu](u_n, v_n).\boldsymbol{n}.$$

  - ⋆ Material derivative of velocity continuity

$$[\frac{\nabla p}{\rho}] = [\frac{(\nabla . \tau)^T}{\rho}].$$

* How to use them ? *

Numerical scheme in the fluid

Predictor-corrector scheme (Chorin-Temam) :

- Prediction (we take $p = 0$)

$$\frac{\boldsymbol{u}^* - \boldsymbol{u}^n}{\Delta t} = \underbrace{-[(\boldsymbol{u} \cdot \nabla)\boldsymbol{u}]^n}_{\text{WENO 5}} + \underbrace{\frac{(\nabla . \tau^n)^T}{\rho}}_{\text{centered second-order}} - \boldsymbol{g}$$

- Resolution of an elliptic equation :

$$\nabla \cdot (\frac{1}{\rho} \nabla p^{n+1}) = \underbrace{\frac{\nabla \cdot \boldsymbol{u}^*}{\Delta t}}_{\text{centered second-order}}$$

- Correction

$$\boldsymbol{u}^{n+1} = \boldsymbol{u}^* - \underbrace{\frac{\Delta t}{\rho} \nabla p^{n+1}}_{\text{centered second-order}}$$

Numerical scheme in the fluid

- Prediction

$$\frac{\boldsymbol{u}^* - \boldsymbol{u}^n}{\Delta t} = -[(\boldsymbol{u} \cdot \nabla)\boldsymbol{u}]^n + \frac{(\nabla.\tau^n)^T}{\rho} - \boldsymbol{g}$$

- Elliptic equation :

$$\nabla \cdot (\frac{1}{\rho} \nabla p^{n+1}) = \frac{\nabla \cdot \boldsymbol{u}^*}{\Delta t}$$

- Correction :

$$\boldsymbol{u}^{n+1} = \boldsymbol{u}^* - \frac{\Delta t}{\rho} \nabla p^{n+1}$$

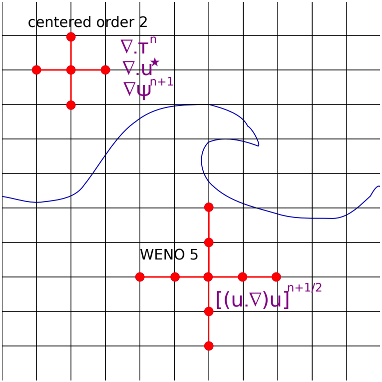

Discretization near the interface

Prediction :

$$\frac{\boldsymbol{u}^* - \boldsymbol{u}^n}{\Delta t} = -[(\boldsymbol{u} \cdot \nabla)\boldsymbol{u}]^n + \frac{(\nabla.\tau^n)^T}{\rho} - \boldsymbol{g}$$

- Diffusion :
  discontinuous velocity derivatives
  $\Rightarrow$ lack of consistency
- Convection :
  WENO 5 naturally adaptative
  continuous velocity
  $\Rightarrow$ less worrying, to a certain extent

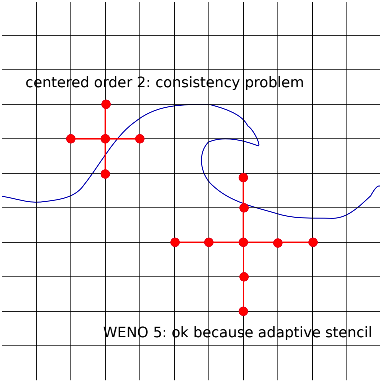

Discretization near the interface

- Elliptic equation :

$$\nabla \cdot (\frac{1}{\rho}\nabla p^{n+1}) = \frac{\nabla \cdot \boldsymbol{u}^*}{\Delta t}$$

Discontinuity for ρ, jump conditions

$\Rightarrow$ lack of consistency

- Correction :

$$\boldsymbol{u}^{n+1} = \boldsymbol{u}^* - \frac{\Delta t}{\rho}\nabla p^{n+1}$$

Discontinuity of ρ and ϕ

$\Rightarrow$ lack of consistency

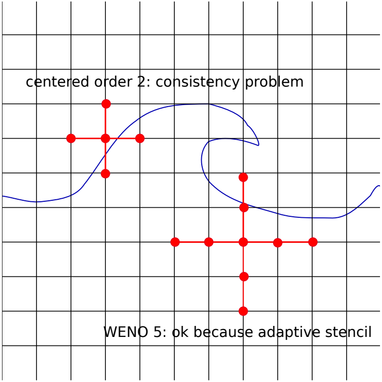

State of the art for methods on cartesian grids

CSF method (Brackbill et al. 91) :
the classical one
regularization of values near the interface, surface tension effect re-formulated as the limit of a volumic force

Methods without regularization :

- VOF methods : Sussman et al, Luo et al., Le Chenadec and Pitsch ...
- Kang, Fedkiw and Liu 2000 : application of Ghost Fluid method
- Raessi and Pitsch 2012 : cut-cell type method

Ghost fluid method

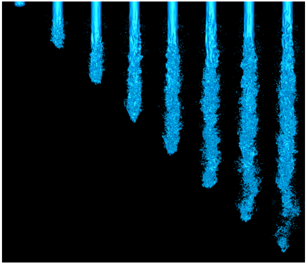

Turbulent atomization of a liquid Diesel jet (Desjardins et al.)

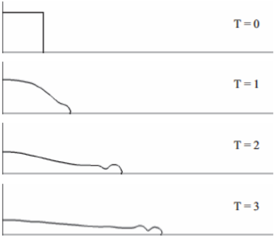

Dam break test case : propagation of interface

⇒ Easy to implement, nice results, but stability issues due to erroneous momentum transfers between fluids

Use of conservative equations for mass and momentum near the interface, solved consistently with the same flux density

$$\frac{\partial \rho}{\partial t} + \nabla \cdot (\rho \boldsymbol{U}) = 0$$

$$\frac{\partial (\rho \boldsymbol{U})}{\partial t} + \nabla \cdot (\rho \boldsymbol{U}\boldsymbol{U}) = -\nabla p + \nabla \cdot \tau + \boldsymbol{F}_B,$$

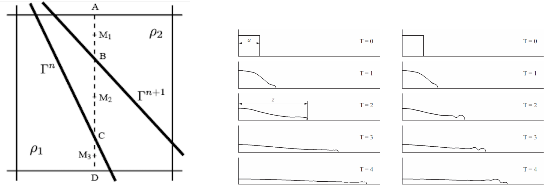

FIGURE: Left : geometrical reconstruction near the interface, right : dam break, comparison between Ghost-Fluid method and conservative methode of Raessi and Pitsch

New method : discretization near the interface

To solve accurately the pressure :

- Creation of interface unknowns for u^* and p on the interface
- Regularization of μ and ρ only to take into account viscous effects
  $\Rightarrow$ no more discontinuity for viscous terms

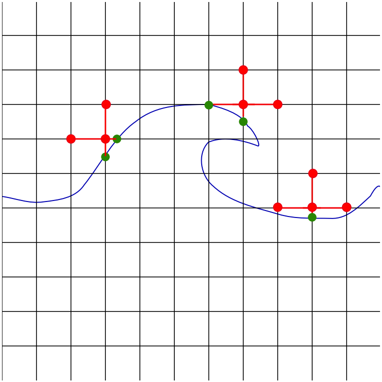

Elliptic problem

- In the fluid :

$$\nabla \cdot (\frac{1}{\rho}\nabla p) = \frac{\nabla \cdot \boldsymbol{u}^*}{\Delta t}.$$

(u^* extrapolated on interface)

- On interface :

$$[p] = \sigma\,\kappa,$$

$$[\frac{\nabla p}{\rho}] = 0.$$

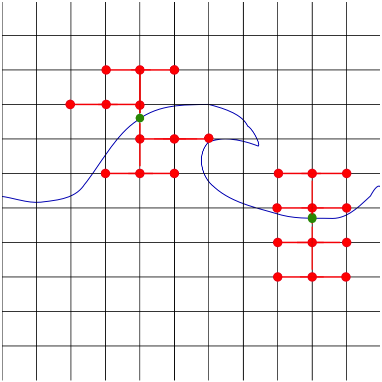

Discretization near the interface

Elliptic problem

- In the fluid :

$$\nabla \cdot (\frac{1}{\rho} \nabla p) = \frac{\nabla \cdot \boldsymbol{u}^*}{\Delta t}.$$

- On interface :

$$[p] = \sigma\, \kappa,$$
$$\text{either } [\frac{p_x}{\rho}] = 0,$$
$$\text{or } [\frac{p_y}{\rho}] = 0.$$

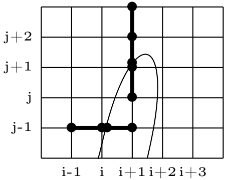

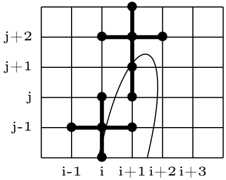

∗ Elimination of interface variables

∗ Convergence analysis valid since the derivatives across the interface are aligned with the axis of the grid

Bubble at rest : parasitic oscillations

- Parasitic oscillations caused by approximated values of the curvature
- More or less amplified by the numerical scheme for the pressure

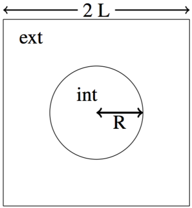

$$\begin{cases} L = 2\ cm, \\ R = 1\ cm, \\ \rho_{int} = 1000\ kg.m^{-3}, \\ \mu_{int} = 10^{-3}\ Pa.s, \\ \rho_{ext} = 1\ kg.m^{-3}, \\ \mu_{ext} = 10^{-5}\ Pa.s, \\ \sigma = 0.1\ N.m^{-1} \end{cases}$$

N	Ghost Fluid method	CSF	new method
16	8.08×10^{-3}	3.55×10^{-2}	5.21×10^{-3}
32	3.42×10^{-4}	3.12×10^{-2}	9.26×10^{-5}
64	5.13×10^{-5}	2.12×10^{-2}	1.36×10^{-5}
128	2.79×10^{-5}	6.44×10^{-3}	2.22×10^{-6}

TABLE: Error in L^∞ norm at time $t = 1$.

Bubble at rest : parasitic oscillations

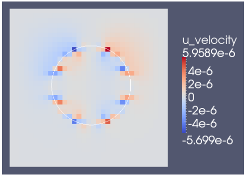

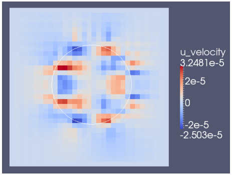

FIGURE: Left : 32* 32 grid, horizontal velocity after 1 iteration, right : horizontal velocity after 1s.

Δx	error L^∞ for VOF (Sussman et al)	error L^∞ for new method
$2.5/16$	$7.3\ 4\times10^{-4}$	$7.48\ \times10^{-5}$
$2.5/\ 32$	$4.5\ \times10^{-6}$	$4.7\ \times10^{-6}$
$2.5/64$	$5.5\ \times10^{-8}$	$1.26\ \times10^{-6}$

Error at non-dimensional time $t = 250$ for the VOF method of Sussman et al. and new method

Small air bubble into water

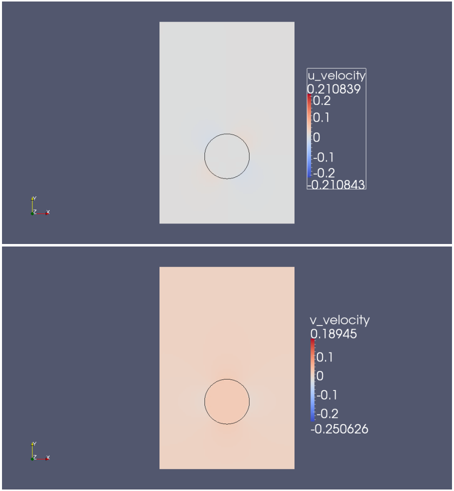

FIGURE: Water : $\rho = 1000$ kg$/m^3$, $\mu = 1,137.10^{-3}$ kg/ms, air : $\rho = 1$kg$/m^3$, $\mu = 1,78.10^{-5}$ kg/ms, $\sigma = 0.0728$ kg$/s^2$, bubble radius $1/300$ m, $Tf = 0.05s$.

Small air bubble into water

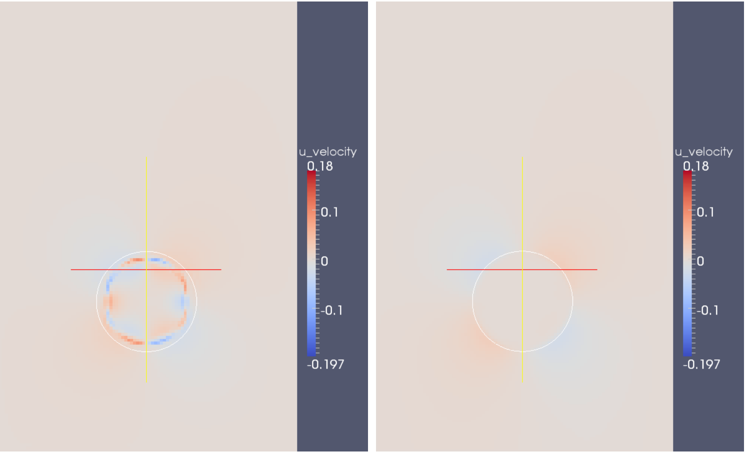

FIGURE: Comparison between CSF method (left) and new method (right)

Larger air bubble into water

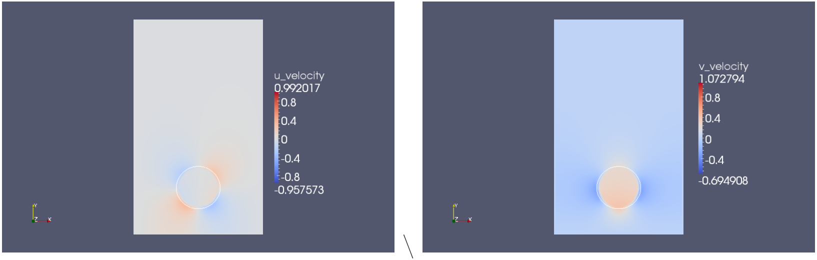

FIGURE: Water : $\rho = 1000$ kg$/m^3$, $\mu = 1,137.10^{-3}$ kg/ms, air : $\rho = 1$kg$/m^3$, $\mu = 1,78.10^{-5}$ kg/ms, $\sigma = 0.0728$ kg$/s^2$, bubble radius 0.025 m

Small water droplet in air

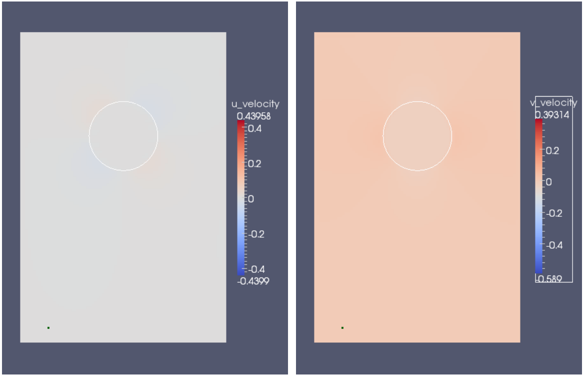

FIGURE: Water : $\rho = 1000$ kg$/m^3$, $\mu = 1,137.10^{-3}$ kg/ms, air : $\rho = 1$kg$/m^3$, $\mu = 1,78.10^{-5}$ kg/ms, $\sigma = 0.0728$ kg$/s^2$, bubble radius $1/300$ m, $Tf = 0.05s$.

Dam break

Water : $\rho = 1000$ kg$/m^3$, $\mu = 1,137.10^{-3}$ kg/ms,
Air : $\rho = 1,226$kg$/m^3$, $\mu = 1,78.10^{-5}$ kg/ms,
$\sigma = 0.0728$ kg$/s^2$, water column $h = 5.715$ cm, domain 40×10 cm

Dam break

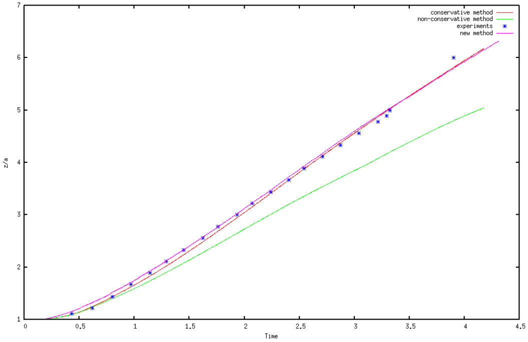

Propagation of front : comparison between the conservative method of Raessi and Pitsch, the Ghost-Fluid method and our new method

Outline

1. Second-order cartesian method for elliptic problems with immersed interfaces
2. Application to incompressible bifluid flows
3. How to preserve high-order level-set along time ? (with F. Luddens and M. Bergmann)

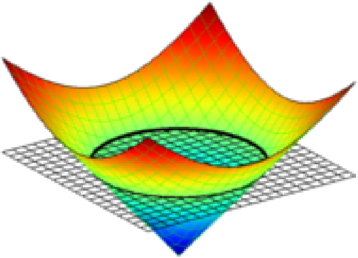

Motivations for a high order level-set

- Better description of the interface
- Mass conservation
- Need of a consistent κ to compute surface tension effects :

$$[p^{n+1}] = \sigma \, \kappa$$

Third-order accuracy needed to compute consistently κ from derivatives of the level-set !

Standard approach

- Transport of ϕ with $\boldsymbol{u}$ (or with an extension velocity) :

$$\phi^* = \phi^n - \Delta t\, \boldsymbol{u}^n \nabla \phi^n,$$

- Every few time steps, re-initialize ϕ^* with :
  - a Fast-Marching algorithm
  - a Fast-Sweeping algorithm
  - a relaxation method

$$\partial_\tau \phi + sign(\phi^*)\,(|\nabla \phi| - 1) = 0,$$
$$\phi_{|\tau=0} = \phi^*.$$

- Very often, RK3-TVD scheme for τ, t, WENO-5 scheme for $\nabla\phi$.

Standard approach

- Transport of ϕ with $\boldsymbol{u}$ (or with an extension velocity) :

$$\phi^* = \phi^n - \Delta t\, \boldsymbol{u}^n \nabla \phi^n,$$

- Every few time steps, re-initialize ϕ^* with :
  - a Fast-Marching algorithm
  - a Fast-Sweeping algorithm
  - a relaxation method

$$\partial_\tau \phi + sign(\phi^*)\,(|\nabla \phi| - 1) = 0,$$
$$\phi_{|\tau=0} = \phi^*.$$

- Very often, RK3-TVD scheme for τ, t, WENO-5 scheme for $\nabla\phi$.

Main problems of standart approach :

- WENO-5 schemes for reinitialization not enough accurate near interface $\Rightarrow$ the interface moves at each reinitalization step
- Cost : too many reinitialization steps ?
- With extension velocities : more accurate but even more costly

To reduce the interface moving

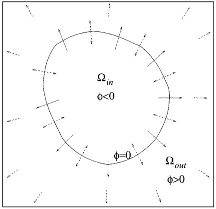

Constatation :
The WENO scheme uses information from the wrong side of the interface

Subcell fix (Russo & Smereka, 2000) :
Use information on interface to modify the scheme (decentering)

Higher order extension (Du Chéné et al. 2008) :

- Far from interface, WENO scheme,
- near interface, decentered ENO scheme, taking into account the interface position

Example : interface with strong gradients

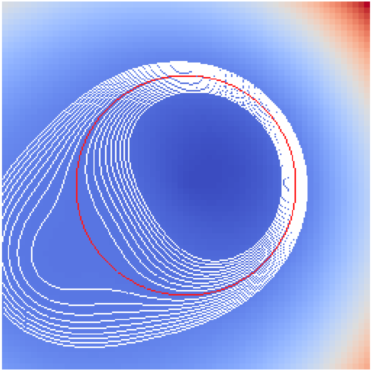

$$d = \sqrt{x^2 + y^2} - r_0$$

$$\phi_0 = \frac{d}{r_0}\left(\epsilon + (x - x_0)^2 + (y - y_0)^2\right)$$

$$\Omega = (-1, 1)^2$$

$$r_0 = 0.5$$

$$\epsilon = 0.1,\ x_0 = -0.7,\ y_0 = -0.4$$

Example : interface with strong gradients

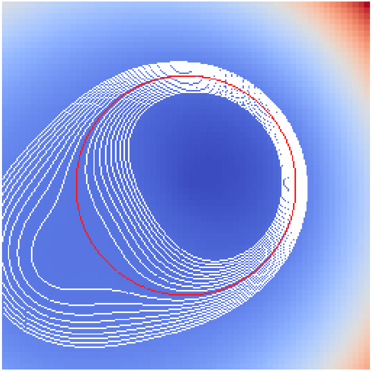

$\frac{1}{h}$	$\Vert\phi_h - d\Vert_{L^1(\Omega)}$ err	coc	$\Vert\phi_h - d\Vert_{L^\infty(B_n)}$ err	coc
20	3.37E-03	-	3.12E-02	-
40	4.25E-04	2.88	1.51E-03	4.22
80	1.10E-04	1.92	2.48E-04	2.56
160	3.19E-05	1.77	2.85E-05	3.09
320	9.43E-06	1.75	3.37E-06	3.06
640	2.57E-06	1.87	6.09E-07	2.46
1280	6.82E-07	1.91	6.98E-08	3.12

Example : interface with strong gradients

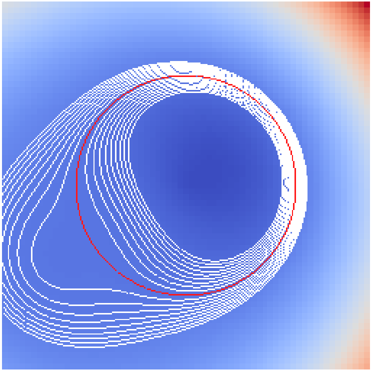

$\frac{1}{h}$	$\|\kappa_h - \kappa\|_{L^\infty(\Gamma)}$ err	coc	N_{it}
20	8.95E-02	-	24
40	4.01E-02	1.12	26
80	1.91E-02	1.05	28
160	9.38E-03	1.01	31
320	4.52E-03	1.05	34
640	2.34E-03	0.95	36
1280	1.18E-03	0.98	38

Coupling with transport

We introduce the quantity $r_g(\nabla\phi) := \| |\nabla\phi| - 1 \|_{L^1(\Omega)}$, and choose a threshold $\delta > 0$.

Algorithm :

- Initialization : with $\phi_0 = d_0$, the signed distance function at interface Γ_0,
- Transport : While $r_g(\nabla\phi) < \delta$, compute the evolution of ϕ with transport equation
- Re-initialization : When $r_g(\nabla\phi) \geq \delta$, re-compute ϕ as the signed distance function d.
  - redistanciation with relaxation in a band around interface
  - second-order fast-sweeping elsewhere

Vortex test case

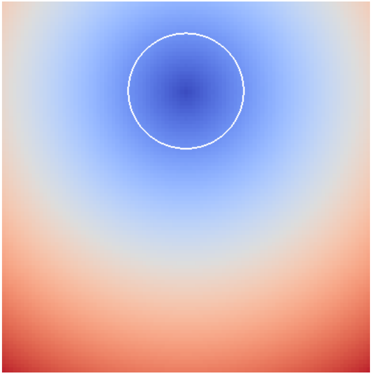

$\Omega = (0,1)^2$

$\phi_{|t=0} = \sqrt{((x-0.5)^2 + (y-0.75)^2)} - 0.15$

$\boldsymbol{u} = \cos\left(\frac{\pi t}{T}\right) \nabla^{\perp}\omega$

$\omega = \sin(\pi x)^2 \sin(\pi y)^2$

$T = 4, t_{fin} = 4$

Γ deforms then goes back to Γ_0 at $t = t_{fin}$.

Vortex test case

Comparison between 4 cases, at time $t = 2$:

1. 5 iterations of relaxation method, every 5 time steps
2. 3 iterations of relaxation method, every time steps
3. new method, with $\delta = 0.1$,
4. new method, with $\delta = 0.01$.

Vortex test case

$\frac{1}{h}$	case 1		case 2		case 3		case 4	
	err.	coc	err.	coc	err.	coc	err.	coc
40	1.82E-01	-	1.18E-01	-	1.47E-01	-	1.22E-01	-
80	5.53E-02	1.69	6.35E-02	0.87	4.63E-02	1.64	4.16E-02	1.53
160	7.07E-02	-0.35	7.62E-02	-0.26	1.51E-02	1.61	1.30E-02	1.66
320	6.56E-02	0.11	9.56E-02	-0.33	4.58E-03	1.71	3.87E-03	1.74
640	1.10E-01	-0.75	2.01E-01	-1.07	3.27E-04	3.80	3.05E-04	3.66

TABLE: Error L^∞ on curvature at $t = 2$

Vortex test case

$\frac{1}{h}$	case 1	case 2	case 3	case 4
40	6.82E-03	1.06E-03	5.67E-03	2.50E-03
80	9.39E-04	2.72E-04	4.06E-04	1.53E-04
160	1.86E-04	2.19E-04	1.88E-05	1.30E-05
320	7.38E-05	1.15E-04	9.66E-07	9.25E-07
640	3.66E-05	6.21E-05	4.30E-08	3.50E-08

TABLE: Volume loss at $t = 2$.

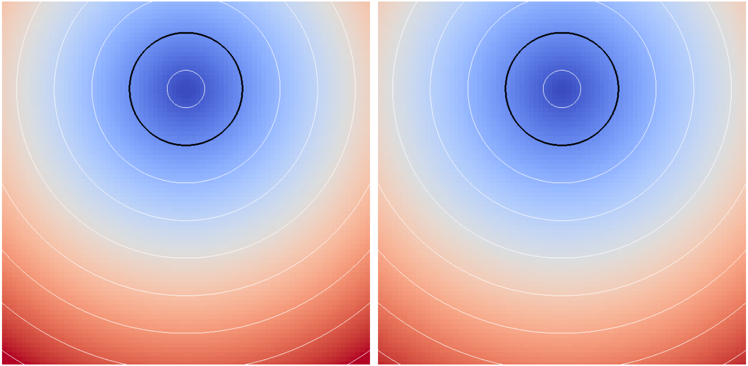

FIGURE: Left : $\delta = 0$ (i.e.redistanciation at time step), right : $\delta = 0.1$. grid 80×80, $dt = dx/8$

Flow around a cylinder

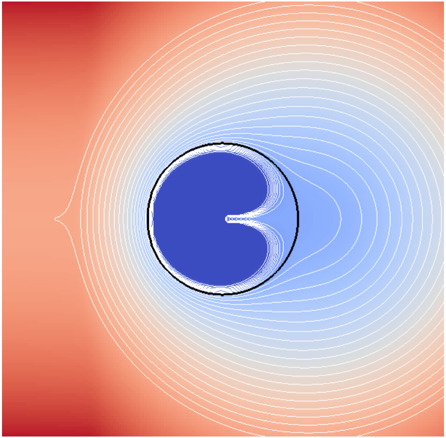

$$\Omega = [-3;3]^2,$$

$$\Gamma_0 = \left\{x^2 + y^2 = 1\right\}, \quad \phi_0 = d_0,$$

$$U_r = \alpha c(r) \left(U_\infty - \frac{1}{r^2} \right) \cos(\theta),$$

$$U_\theta = -\alpha c(r) \left(U_\infty + \frac{1}{r^2} \right) \sin(\theta),$$

$$c(r) = \min \left(1, \frac{r}{0.5} \right)^3,$$

$$U_\infty = 1,$$

α such that $\|\boldsymbol{U}\|_{L^\infty(\Omega)} = 1$,

$$t_{fin} = 6.$$

Flow around a cylinder

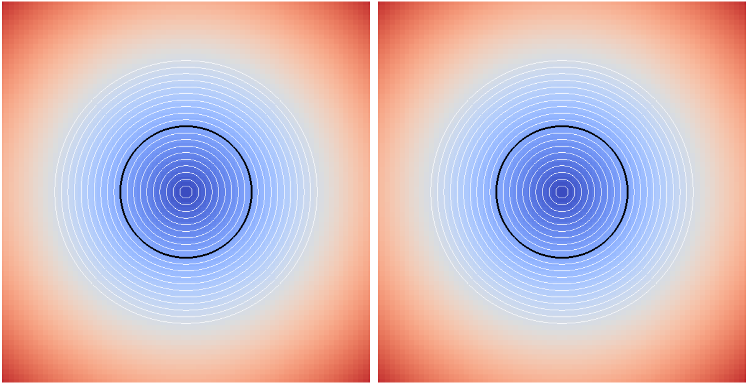

FIGURE: Left : $\delta = +\infty$ (i.e. no redistanciation), right : $\delta = 0.1$, grid 80×80

$\frac{1}{h}$	$\delta = 0.01$		$\delta = 0.1$		$\delta = +\infty.$	
	err.	coc	err.	coc	err.	coc
40	7.24E-02	-	8.35E-02	-	1.40E+00	-
80	3.91E-02	0.87	1.68E-02	2.27	2.15E+00	-0.61
160	9.71E-03	1.99	5.09E-03	1.71	3.53E+00	-0.71
320	3.66E-03	1.40	2.51E-03	1.01	8.22E+01	-4.52
640	2.51E-03	0.54	1.88E-03	0.42	1.57E+02	-0.93

TABLE: $\|\kappa_h - \kappa\|_{\infty(\Gamma)}$ at $t = 6$ and convergence order.

Rising of a large air bubble into water : new redistanciation

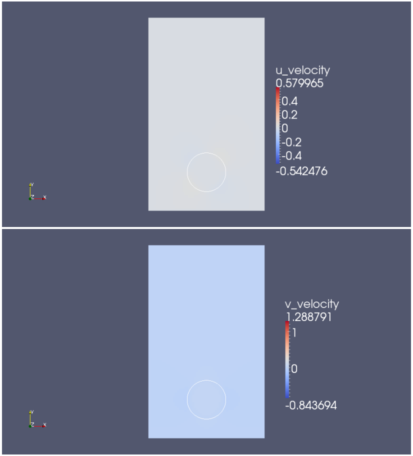

FIGURE: Water : $\rho = 1000$ kg$/m^3$, $\mu = 1,137.10^{-3}$ kg/ms, air : $\rho = 1$kg$/m^3$, $\mu = 1,78.10^{-5}$ kg/ms, $\sigma = 0.0728$ kg$/s^2$, bubble radius 0.025 m

Rising of a large air bubble into water : new redistanciation

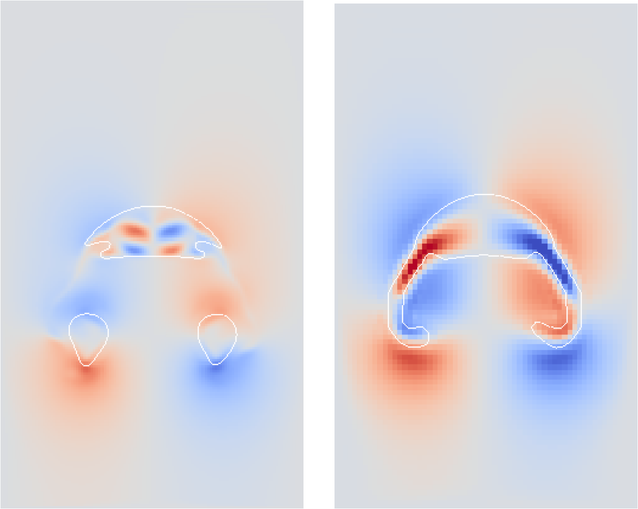

FIGURE: Water : $\rho = 1000$ kg$/m^3$, $\mu = 1,137.10^{-3}$ kg/ms, air : $\rho = 1$kg$/m^3$, $\mu = 1,78.10^{-5}$ kg/ms, $\sigma = 0.0728$ kg$/s^2$, bubble radius 0.025 m

Conclusion

- New cartesian method for incompressible bifluid flows with high density ratios :
  - with second-order pressure resolution
  - compromise between accuracy and simplicity
- To obtain a third-order level-set method along time :
  DO NOT use redistanciation every few time steps !

In the future :

- Implementation in NasCar code
- Application to air-water interface + floating solid
- Development of an incremental form
- Comparisons with other families of methods : front-tracking, VOF, phase-field...